Vol 18 No 11, November 2009
1674-1056/2009/18(11)/4865-05

Chinese Physics B

© 2009 Chin. Phys. Soc.
and IOP Publishing Ltd

Tapered dielectric structure in metal as a wavelength-selective surface plasmon polariton focuser*

Zhang Yang(张 洋), Zhao Qing(赵 清), Liao Zhi-Min(廖志敏), and Yu Da-Peng(俞大鹏)†

State Key Laboratory for Mesoscopic Physics, and Electron Microscopy Laboratory, School of Physics, Peking University, Beijing 100871, *China*

(Received 19 April 2009; revised manuscript received 30 May 2009)

Symmetric tapered dielectric structures in metal have demonstrated applications such as the nanofocusing of surface plasmon polaritons, as well as the waveguiding of V-channel polaritons. Yet the fabrication of smooth-surfaced tapered structure remains an obstacle to most researchers. We have successfully developed a handy method to fabricate metal-sandwiched tapered nanostructures simply with electron beam lithography. Though these structures are slightly different from conventional symmetric V-shaped structures, systematic simulations show that similar functionality of surface plasmon polariton nanofocusing can still be achieved. When parameters are properly selected, wavelength-selective nanofocusing of surface plasmon polaritons can be obtained.

Keywords: tapered structure, surface plasmon, focusing, finite-difference time-domain
PACC: 4110H, 7320J, 4282

One of the major hot topics in nano-optics is localized plasmons in metallic structures. These structures offer the unique opportunity to confine electromagnetic energy in a limited space. Therefore, the ability to deliver electromagnetic radiation on a nanoscale is crucial to nano-optics. The focusing of surface plasmon polaritons (SPPs) has diverse applications in sub-wavelength waveguiding,[1] nanolithography,[2,3] and sensing.[4] Besides, large electromagnetic fields allow the enhancement of nonlinear optical effects.[5−7] A number of metallic structures have been designed to focus SPPs,[1−12] among which tapered air wedges in metal have drawn a lot of attention due to their excellent spatial confinement.[13−15] They can also function as V-channel plasmon polariton (CPP) waveguides,[16−20] and promise relatively weak dissipation, single-mode operation, and 100% transmission through sharp bends. When two half-space metal–vacuum interfaces are close enough, SPPs are coupled into symmetric as well as antisymmetric gap plasmon polariton (GPP) modes.[13−15] Symmetric GPPs modes can exist in an infinite small gap, producing prominent electromagnetic field enhancement.

Most previous work has focused on plasmon propagation towards the tip in a strictly symmetric tapered air wedge in metal.[13−15] However, only theoretical calculations have been performed and no such structures in the strict sense have been fabricated. In the present article, we propose a new type of tapered structure which is slightly different from the conventional symmetric V-shaped structure. In contrast to various complex techniques developed to fabricate tapered structures,[21−24] by our method the tapered structures are easily fabricated simply with electron beam lithography (EBL).[25] Besides, surface roughness can be limited to the same level as that of a polymethyl methacrylate (PMMA) surface, regardless of the deposition techniques, which minimizes the scattering loss of the SPPs. Simulations show that, despite their asymmetry, these structures still achieve nanoscale SPP focusing and have wavelength selectivity if structure parameters are appropriately selected.

Figure 1 is a typical cross-sectional profile of the tapered structure fabricated by our method. In our simulation, the smoothly bent upper surface of the structure is simulated by joining two arcs which are tangential to each other. Four parameters are introduced to characterize the tapered structure: the maximum gap, the minimum gap, the slope angle, and the extension length. The maximum gap is the spacing at the wide opening. The minimum gap is the spacing of the region where the focused plasmons finally pass through. The slope angle

*Project supported by the National Natural Science Foundation of China (Grant Nos 90606023, 10574003 and 20731160012), a National 973 Project (Grant No 2007CB936202 and 2009CB623703) and MOST from China's Ministry of Science and Technology and Hong Kong's NSFC/RGC Joint Research Scheme (Project No N_HKUST615/06).
†Corresponding author. E-mail: yudp@pku.edu.cn

is the maximum slope of the tapered structure. The extension length is the distance from the tangent point of the upper surface to the opening end.

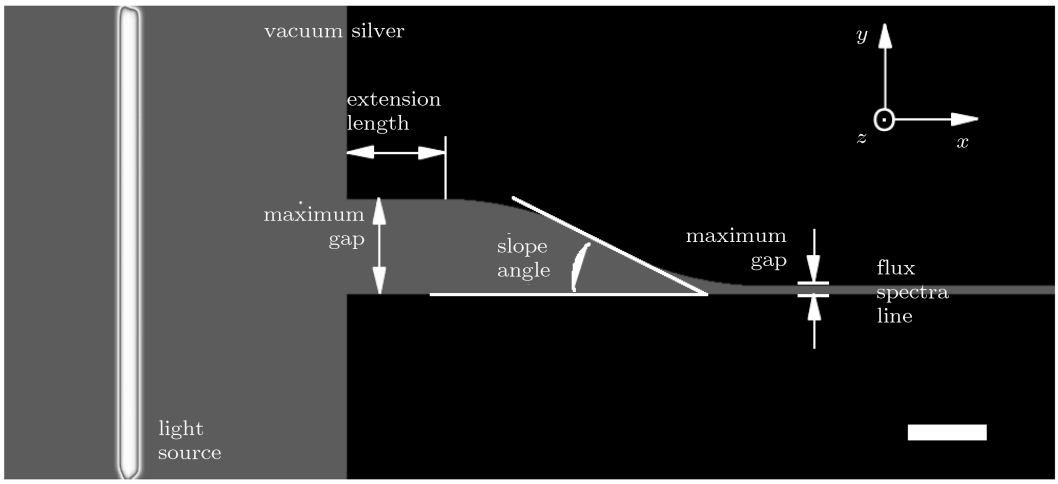


Fig.1. A typical cross-sectional profile of a silver-sandwiched tapered structure fabricated by our method. The scale bar represents 500 nm, where the schematic presentation of the four parameters which are used to characterize the tapered structure, the position of the light source and the flux spectral line are also indicated.

The finite-difference time-domain method (FDTD) is one of the most popular techniques due to its easy implementation and flexibility, and it has been used to simulate dispersive materials.[26] In the present article, it is used to simulate SPP propagation in metallic structures. We assume that the dielectric function of silver is described by the Drude model

$$\varepsilon(\omega) = \varepsilon_\infty - \omega_{\rm p}^2[\omega(\omega - {\rm i}\,\Gamma)]^{-1}. \qquad (1)$$

In the simulation, we employ the following parameters: $\varepsilon_\infty = 3.7$, $\omega_{\rm p} = 13673$ THz and $\Gamma = 27.35$ THz.[27] The parameters were calculated by Sönnichsen based on experimental data of reflection and transmission of 25–50 nm thick silver films obtained from a wavelength range of 0.188–1.9 μm by Johnson and Christy.[27,28]

In simulation by the FDTD, perfectly matched layers (PML) are used as boundaries in both x and y directions. The size of the simulation region is 6 μm×3 μm and the space discretization step is $\Delta r =$ 100 nm/15, i.e. 6.66 nm. The SPPs are excited by a line Gaussian light source placed to the left of the opening, parallel to the y axis, with TM polarization (magnetic field along the z axis), and a flux spectral line is placed 500 nm to the right of the closing end to collect spectra (Fig.1). Then 6000 simulation steps, each of which is equal to $\Delta t = \Delta r/2c = 1.11\times10^{-17}$ s, are performed, allowing the initial field to evolve, and the next 6000 simulation steps are recorded. Light is scattered at the opening end and transformed into SPPs propagating along the two surfaces. Since the gap between the two surfaces is large at the opening, the SPPs propagate independently of each other. The slope is very smooth, so very little scattering happens. But as the gap shrinks, the SPPs on the two surfaces are coupled into GPPs, accompanied by reflection of the SPPs at the tapering part.

Electromagnetic field enhancement is the main feature of SPP focusing. We define the enhancement factor spectra as the transmission spectra collected at the narrow gap of the structure divided by the spectra collected from a flux spectra line with width identical to the narrow gap without the structure. The enhancement factor represents the average enhancement of the density of energy, or Poynting vector length, at the narrow gap. In the following, the effects of all four parameters on SPP focusing are systematically examined.

The minimum gap determines the scale of the limited space where GPPs are confined, thus it is very important. We fix the maximum gap at 600 nm and the slope angle at 30°, without extension. As shown in Fig.2, by varying the minimum gap, the enhancement factor increases dramatically as the minimum

gap decreases, especially below 100 nm. When the minimum gap is reduced from 100 nm to 50 nm, the enhancement factor leaps from ∼5 to ∼10. Stronger field enhancement is expected if we further reduce the minimum gap. Therefore, to achieve significant field enhancement, the minimum gap has to be sufficiently small at the tip of the tapered structure. Our fabrication technique can easily ensure the minimum gap below 50 nm. At the same time, oscillation in the enhancement spectra becomes evident as the minimum gap decreases.

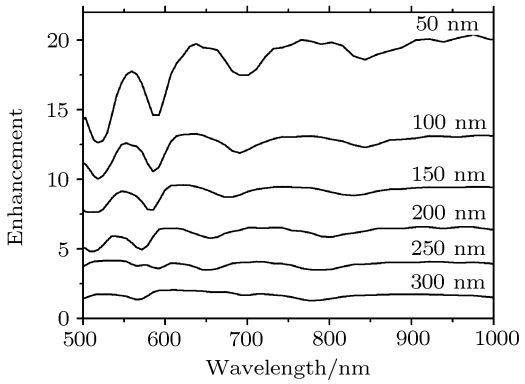


Fig.2. Simulated enhancement spectra with varying minimum gaps of 50, 100, 150, 200, 250 and 300 nm respectively (from top to bottom), when the maximum gap is fixed at 600 nm, and the slope angle at 30^o, without extension. The individual spectra are separated by 2 from each other for viewing.

The oscillation in the spectra might be deriven from two sources. One is from resonance in the waveguiding process. The reflections of the SPPs at the opening end and the closing end could provide the possibility of plasmon resonance. This has been detected by Miyazaki and Kurokawa in the case of GPPs,[29] where absorption dips in the reflection spectra of the GPP resonant cavities were observed. The other is the consequence for antisymmetric GPPs to fail to pass through the narrow gap. If the magnetic fields in the incident plasmons are in antiphase, the resultant plasmon will be antisymmetric, which cannot exist in narrow gaps. The difference in path along the two surfaces could produce phase mismatch, thereby producing an antisymmetric plasmon which cannot pass through the narrow gap. In this case, however, the path difference lies below 300 nm, which is insufficient to produce prominent phase mismatch variance. We believe that the first source is mainly responsible for the oscillation in the enhancement factor, which is confirmed by our further simulations.

To find out how this oscillation in the spectra happens, we examine the distribution of the average energy density in the structure with a minimum gap of 50 nm, by using light sources of two different wavelengths: one is 590 nm, corresponding to the dip in the spectrum; the other is 640 nm, corresponding to the peak in the spectrum. Both structures have exhibited nanofocusing of SPPs at the narrow gap, where energy density is high. This structure shows stronger nanofocusing at the 640 nm wavelength than at the 590 nm wavelength. In the case of the 640 nm light source (Fig.3(b)), electromagnetic energy density spreads uniformly on the surface, except for the bright spot in the centre of the tapering part, where the SPPs from the two surfaces meet in identical phase. No standing waves can be seen in the wide gap. But in the case of the 590 nm light source (Fig.3(a)), energy density distribution is uneven and shows a certain pattern in the wide gap, indicating the existence of standing waves. It can be inferred that the wide-gap segment also acts as a resonant cavity of the SPPs between the opening and the closing ends.

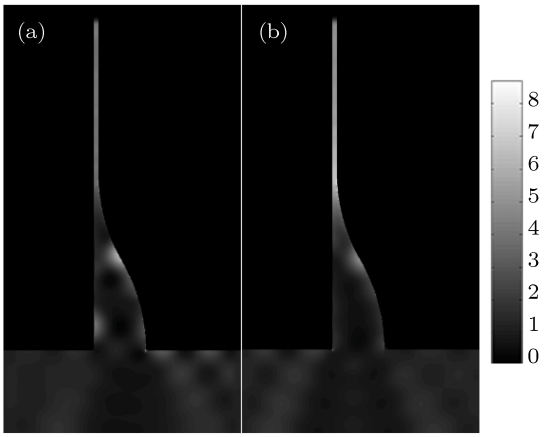


Fig.3. Simulated distribution of the average electromagnetic energy density when the wavelengths of the incident light are 590 (a) and 640 nm (b).

To further confirm our speculation that the cavity mode in the wide-gap segment is the main cause of oscillation in the spectra, we vary the extension length of the structure, thus we vary the length of the resonant cavity. The length of the resonant cavity is closely related to the oscillation of the spectra. As indicated by the formula

$$k \times l = n \times \pi, \tag{2}$$

where k is the wavevector of the SPPs, l is the resonant cavity length, and

$$k_n - k_{n-1} = \frac{\pi}{l}, \tag{3}$$

the longer the resonant cavity is, the more frequent the oscillation will be. Figure 4 shows the general trend as expected based on our assumption. As the resonant cavity becomes longer, the oscillation in the enhancement factor becomes more frequent, and the gaps between the dips shorten.

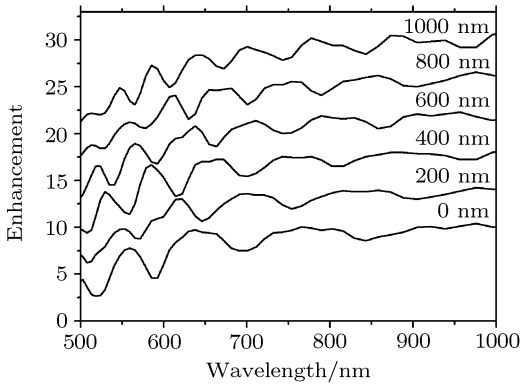


Fig.4. Simulated enhancement spectra for different extension lengths, i.e. 0, 200, 400, 600, 800 and 1000 nm (from bottom to top), with the maximum gap fixed at 600 nm, the minimum gap at 50 nm, the slope angle at 30°. The individual spectra are separated by 5 from each other for viewing.

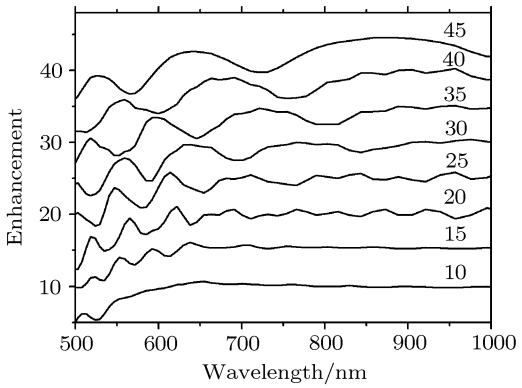


Fig.5. Simulated enhancement spectra for different slope angles, i.e. 10, 15, 20, 25, 30, 35, 40 and 45° (from bottom to top), with the maximum gap fixed at 600 nm, and the minimum gap at 50 nm, without extension. The individual spectra are separated by 5 from each other for viewing.

The influence of the slope angle is also analysed. We fix the maximum width at 600 nm and the minimum width at 50 nm, without extension. By varying the slope angle between 10° and 45°, we obtain strikingly different enhancement-factor spectra. As shown in Fig.5, at small angles, the oscillation is weak and the spectrum is scattered with frequent dips. In the case of a 10° slope angle, no obvious oscillation can be identified. At large angles, the oscillation is stronger and the enhancement-factor spectrum dips less. This can be explained by both the length of the resonator and the reflectivity at the closing end. As the slope angle decreases, the length of the resonator increases. Correspondingly, the gaps between the dips in the spectrum are shortened. On the other hand, as the slope angle decreases, reflection at the closing end decreases,[10,11] and SPPs are more effectively coupled into the GPPs in the narrow gap. In other words, the tapered structures turn into a GPP coupler as the slope angle decreases.

The effect of varying the maximum gap is also examined. The minimum gap is fixed at 50 nm, and the slope angle is fixed at 30°, without extension. As we show in Fig.6, the enhancement factor increases with the maximum gap, especially for large wavelengths. In the meantime, oscillation in the enhancement-factor spectrum becomes obvious and frequent as the maximum gap becomes larger. This can be readily explained by the aforementioned theory. As the maximum gap becomes larger, the resonator lengthens, thereby producing more frequent oscillation. Another thing we should pay attention to is that SPP resonance

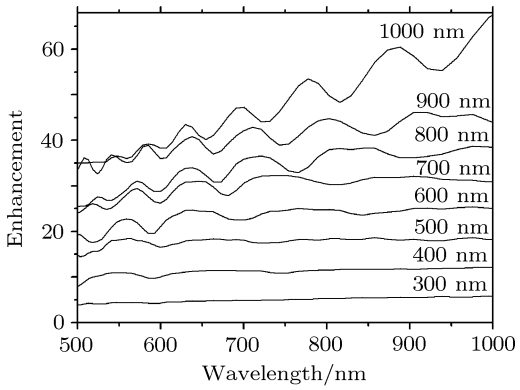


Fig.6. Simulated enhancement spectra for maximum gaps of 300, 400, 500, 600, 700, 800, 900 and 1000 nm (from bottom to top), with minimum gaps fixed at 50 nm, the slope angle at 30°, without extension. The individual spectra are separated by 5 from each other for viewing.

happens when independent SPPs are reflected at the closing end. This does not hold when the maximum gap is small compared with the SPP penetration depth in air. In this case, only GPPs instead of SPPs exist in the wide gap. The coupling of SPPs on the two surfaces strengthens as the penetration depth in air increases, i.e. the wavelength increases. As a result, oscillation at long wavelengths weakens due to the closing gap being insufficient to reflect GPPs. As the maximum gap widens, independent SPPs with longer wavelengths can be accommodated in the wide gap,

providing the basis for the resonances at longer wavelengths.

In conclusion, we have successfully fabricated various tapered dielectric structures in silver which can be used as SPP focusers. FDTD simulations show that SPP focusing with an enhancement factor of over 10 can be achieved when the minimum gap is below 50 nm. Through these asymmetric structures, the SPPs can be well coupled into the GPPs in the narrow gap. The wide-gap segment can function as SPP resonant cavities when the slope angle is large. At large slope angles, only the SPPs that are not at the resonant frequency can be effectively focused and coupled into GPPs in the narrow gap.

References

[1] Yin L L, Vlasko-Vlasov V K, Pearson J, Hiller J M, Hua J, Welp U, Brown D E and Kimball C W 2005 *Nano Lett.* **5** 1399

[2] Fang N, Lee H, Sun C and Zhang X 2005 *Science* **308** 534

[3] Fang L, Du J L, Guo X W, Wang J Q, Zhang Z Y, Luo X G and Du C L 2008 *Chin. Phys.* B **17** 2499

[4] Homola J, Yee S S and Gauglitz G 1999 *Sens. Actuators* B **54** 3

[5] Verhagen E, Kuipers L and Polman A 2007 *Nano Lett.* **7** 334

[6] Shen H, Cheng B L, Lu G W, Wang W T, Guan D Y, Chen Z H and Yang G Z 2005 *Chin. Phys.* **14** 1915

[7] Wang W T, Yang G, Chen Z H, Zhou Y L, Lü H B and Yang G Z 2002 *Chin. Phys.* **11** 1324

[8] Liu Z, Steele J M, Srituravanich W, Pikus Y, Sun C and Zhang X 2005 *Nano Lett.* **5** 1726

[9] Offerhaus H L, van den Bergen B, Escalante M, Segerink F B, Korterik J P and van Hulst N F 2005 *Nano Lett.* **5** 2144

[10] Radko I P, Bozhevolnyi S I, Evlyukhin A B and Boltasseva A 2007 *Opt. Express* **15** 6576

[11] Ropers C, Neacsu C C, Elsaesser T, Albrecht M, Raschke M B and Lienau C 2007 *Nano Lett.* **7** 2784

[12] Stockman M I 2004 *Phys. Rev. Lett.* **93** 137404

[13] Gramotnev D K 2005 *J. Appl. Phys.* **98** 104302

[14] Pile D F P 2006 *Appl. Phys. Lett.* **89** 041111

[15] Pile D F P and Gramotnev D K 2004 *Opt. Lett.* **29** 1069

[16] Novikov I V and Maradudin A A 2002 *Phys. Rev.* B **66** 035403

[17] Gramotnev D K and Pile D F P 2004 *Appl. Phys. Lett.* **85** 6323

[18] Bozhevolnyi S I, Volkov V S, Devaux E and Ebbesen T W 2005 *Phys. Rev. Lett.* **95** 046802

[19] Volkov V S, Bozhevolnyi S I, Devaux E, Laluet J Y and Ebbesen T W 2007 *Nano Lett.* **7** 880

[20] Bozhevolnyi S I, Volkov V S, Devaux E, Laluet J Y and Ebbesen T W 2006 *Nature* **440** 508

[21] Hung K Y, Tseng F G and Chou H P 2005 *Microsyst. Technol.* **11** 365

[22] Kim K T and Hwangbo S 2005 *Sens. Actuators* A **120** 59

[23] Nock V and Blaikie R J 2008 *Microelectron. Eng.* **85** 1077

[24] Waits C M, Modafe A and Ghodssi R 2003 *J. Micromech. Microeng.* **13** 170

[25] Zhang Y and Yu D P 2009 *Chin. Phys. Lett.* **26** 088101

[26] Pernice W H P, Payne F P and Gallagher D F G 2006 *Opt. Quantum Electron.* **38** 843

[27] Saj W M 2005 *Opt. Express* **13** 4818

[28] Johnson P and Christy R 1972 *Phys. Rev.* B **6** 4370

[29] Miyazaki H T and Kurokawa Y 2006 *Phys. Rev. Lett.* **96** 097401